ISSN 1392–1207. MECHANIKA. 2016 Volume 22(5): 359–365

# Flow stress behaviour and constitutive model of 7055 aluminium alloy during hot plastic deformation

**Zhang Tao*, Wu Yun-xin*, Gong Hai**, Shi Wen-ze*, Jiang Fang-min***

**Central South University, State Key Laboratory of High Performance Complex Manufacturing, School of Mechanical and Electrical Engineering, Nonferrous Metal Oriented Advanced Structural Materials and Manufacturing Cooperative Innovation Center Changsha 410083, China, E-mail: 297zhangtao@163.com*

***Central South University, State Key Laboratory of High Performance Complex Manufacturing, School of Mechanical and Electrical Engineering, Nonferrous Metal Oriented Advanced Structural Materials and Manufacturing Cooperative Innovation Center Changsha 410083, China, E-mail: gonghai@csu.edu.cn corresponding author*

crossref http://dx.doi.org/10.5755/j01.mech.22.5.12527

## 1. Introduction

Aluminium alloy plates with high strength and high toughness are widely used in main frames, wing boxes, stringers and other key components of aircraft. 7055 is an ultra-high strength aluminium alloy developed by Alcoa Company in the United States, which was used in the aircraft airfoil of Boeing777.Through the use of T77 heat treatment, the stress corrosion resistance of the alloy can be improved without reducing the strength of the alloy [1]. The use of aluminium alloy plates makes about 1400 pound reduction compared with the designed mass in B777[2].

Material flow behaviour during hot plastic deformation is complex, which consists of two processes: work hardening and dynamic softening and they varied with the changes of deformation temperatures and strain rates. Therefore, the understanding of flow behaviour at hot compression provides guidance for the optimum metal forming processes (hot rolling, forging and extrusion). As deformation temperature and strain rate play a vital role in the flow stress during hot deformation, most researchers use the constitutive equations containing the strain rate and temperature to describe the relationship between the flow stress and these two factors [3, 4]. In the past, many investigations have been carried out on the flow properties at high temperature, but mainly focused on fatigue resistance, corrosion resistance, quenching sensitivity and mechanical properties during heat treatment process [5-9]. Lin [10, 11] analyzed the flow behaviour at high temperature of 42CrMo steel and established the constitutive equation. ZHANG [12] and YAN [13] analyzed flow stress characteristics of the 7 series aluminium alloy during two processes of work hardening and dynamic softening at high temperature deformation. Arrhenius constitutive equations are widely used to describe the relationship between peak flow stress and temperature and strain rate by Zener-Hollomon parameter, the relationship between flow stress and strain is not taken into account. However, from the true stress-strain curves, the change of strain will change the flow stress. Therefore, the Arrhenius constitutive equations should be modified and the effect of strain on the variation of the flow stress should also be taken into consideration to acquire a more accurate constitutive equation. Artificial neural network models and Arrhenius-type constitutive equations [14-15] had been built by many researchers for steel, titanium alloy and other alloy. Other work for aluminium alloy focused on 7085 and 7050 [16-17], which had been developed for a long time. However, modified Arrhenius constitutive equations for 7055 aluminium alloy were rarely published. The hot deformation behaviour of 7055 aluminium alloy needs to be further studied to establish the optimum formation process parameters as 7055 is a kind of relatively new aviation material. In this study, a modified constitutive equation considering strain compensation is built: successive approximation method is used to obtain the accurate stress exponent *n*, which is an important parameter in the constitutive equation. Then, polynomial fitting is used to describe the relationship between material parameters and true strain. As a result, the relationship between flow stress and temperature, strain and strain rates can be described by the constitutive equation considering strain compensation. Finally, the validity of the modified constitutive models was examined over all the temperatures and strain rates by the comparison of the experimental and calculated results.

## 2. Experiments and results

The material is 7055 aluminium alloy ingot casting after homogenization treatment and its compositions (wt.%)6.7Zn-2.6Mg-2.6Cu-0.15Fe-0.13Zr-0.12Si-0.06Ti.

The homogenization treatment process was conducted as follows: the material was heated to 470°C from room temperature and held for 24 hour to obtain heat balance between the surface and the center, then cooled down with the heating furnace. Cylindrical specimens were machined with a diameter of 10 mm and a height of 15 mm. The hot compression tests were conducted on Gleeble-3180 thermo-simulation machine. Each specimen was heated to the deformation temperature at a rate of 5°C/s and held for 3 min at isothermal conditions, then compressed with different strain rates and quenched immediately after the deformation. The reduction in height is 60% in the end and the true strain is 0.693. In order to reduce the frictions between the specimens and die, lubricants and graphite flakes were added to the flat surface of the specimens in the four different temperatures (300, 350, 400 and 450°C) and four different strain rates (0.01, 0.1, 1 and 10 $s^{-1}$). According to industrial hot rolling parameters of 7 series aluminium alloy, the hot compression temperatures are 300, 350, 400 and 450, the strain rates are 0.01, 0.1,1 and 10 $s^{-1}$.

True stress-strain curves of 7055 aluminium alloy under different compression conditions are depicted in Fig. 1. It is obvious that the true stress is sensitive to deformation temperature and strain rate. The flow stress increases with the increase of strain rate and decreases with the increase of temperature. The stress-strain curve can be divided into three stages: Stage (Work hardening stage), Stage (Transition stage), Stage (Steady stage). In Stage, the hardening rate is higher than the softening rate and the flow stress increases rapidly with the small increase of the strain. This is because the dislocation is significantly increased resulting from the appearance of a large number of dislocation tangles and cellular substructures in the initial deformation stage. In Stage, there is a competition between two process of work hardening and dynamic softening. As a result, the flow stress is increased while the rate of the increase is decreased. The stored energy accumulated in Stage provides a driving force for dislocation movement. Dynamic recovery, even dynamic recrystallization when dislocation exceeds critical dislocation occurs in this stage, which reduces the increasing rate of the flow stress. In Stage, work hardening and dynamic recovery and dynamic recrystallization produce to achieve a balance and the flow stress tends to a steady-state value.

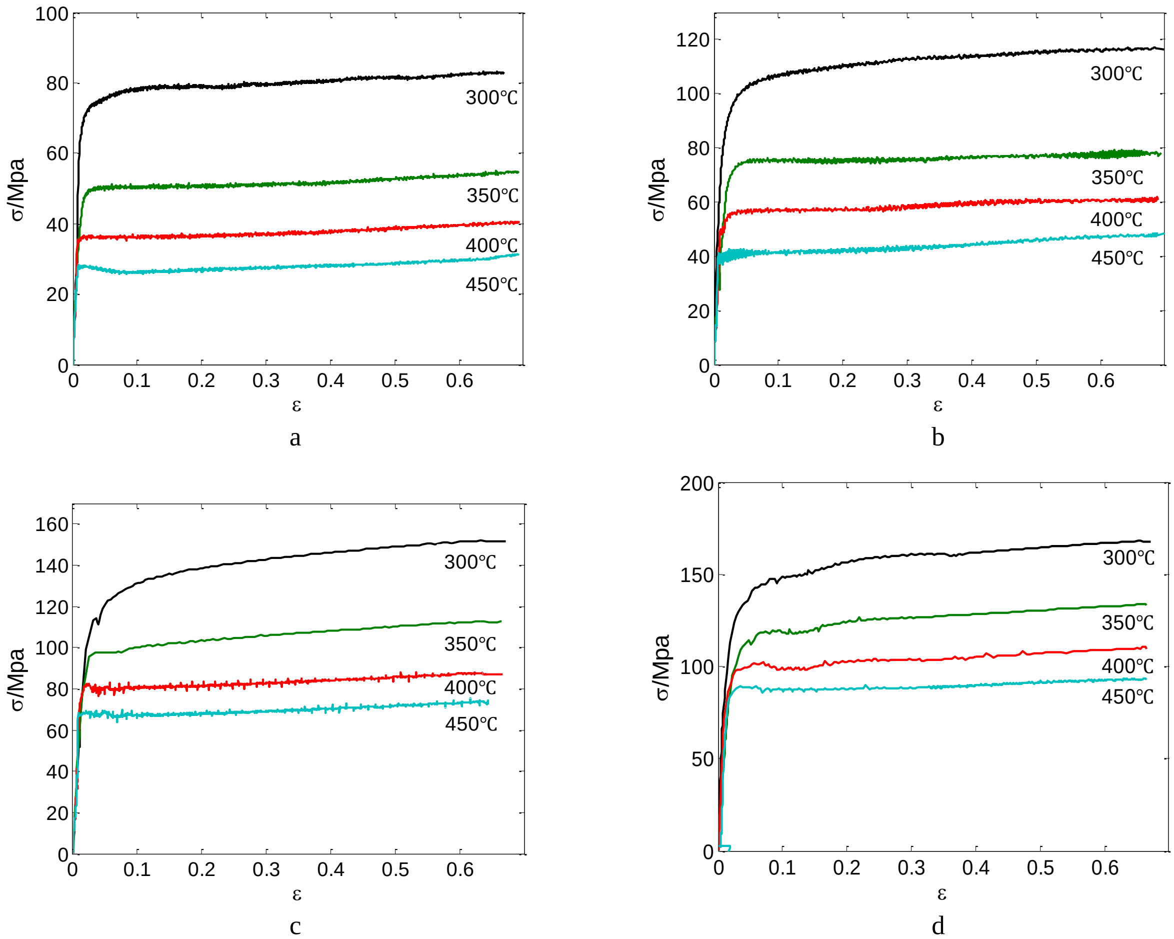


Fig. 1 True stress-strain curves of 7055 aluminium alloy for different conditions a - $\dot{\varepsilon}$ = 0.01 $s^{-1}$; b - $\dot{\varepsilon}$ = 0.1 s-1; c - $\dot{\varepsilon}$ = 1 $s^{-1}$; d - $\dot{\varepsilon}$ = 10 $s^{-1}$

### 3. Constitutive equations

The Arrhenius equation proposed by Sellars and Tegart is widely used to describe the relationship between flow stress and Zener-Hollomon parameter, which represents the effects of the strain rates and temperatures on the hot compression behaviours. $F(\sigma)$ is a function of the flow stress and consists of different forms of expression under different stress levels, as shown in Eqs. (1)-(3), where $\dot{\varepsilon}$ ($s^{-1}$) is the strain rate, $Q_{act}$ (J/mol) the activation energy, $R$ (8.314 J $K^{-1}$ $mol^{-1}$), $T$ (K) the absolute temperature, $\sigma$ (MPa) the flow stress, $A$, $\alpha$ and $n$ are material constants, $\alpha = \beta / n$.

$$Z = \dot{\varepsilon}\, exp\left(\frac{Q_{act}}{RT}\right); \quad (1)$$

$$\dot{\varepsilon} = AF(\sigma)\, exp\left(-\frac{Q_{act}}{RT}\right); \quad (2)$$

$$F(\sigma) = \begin{cases} \sigma^n & (\alpha\sigma < 0.8); \\ exp(\beta\sigma) & (\alpha\sigma > 1.2); \\ \left[sinh(\alpha\sigma)\right]^n & (for\ all\ \sigma). \end{cases} \quad (3)$$

3.1. Successive approximation method

It is commonly known that the effect of strain on flow stress will not be considered in Eqs. (2) and (3). The following is taking the peak flow stress as an example to acquire the material parameters. Stress exponent is an important parameter and its accuracy has a significant effect on the validity of the constitutive equation. Therefore, n was fitted in each step by successive approximation method to reduce the error caused by regression analysis, as shown in Fig. 2.

Step 1: For low stress level ($\alpha\sigma < 0.8$) and high stress level ($\alpha\sigma > 1.2$), substituting $F(\sigma)$ into Eqs. (2), taking the logarithm of both sides, then give:

$$ln(\dot{\varepsilon})=n\,ln(\sigma)+ln(A)-\frac{Q}{RT}\,; \tag{4}$$

$$ln(\dot{\varepsilon})=\beta\sigma+ln(A)-\frac{Q}{RT}\,. \tag{5}$$

Fig. 3 shows the relationship between $ln(\dot{\varepsilon})$ - $ln(\sigma)$ and $ln(\dot{\varepsilon})$ - $\sigma$. The value of $n_1$ and $\beta$ can be obtained from the average slope of the four lines by least square method. The mean value of $n_1$ and $\beta$ were computed as 6.694 and 0.0988, resepectively, $\alpha = \beta / n_1 = 0.0147$.

Step 2: For the all stress level, the relationship between $ln(\dot{\varepsilon})$ - $ln[sinh(\alpha\sigma)]$ and $ln[sinh(\alpha\sigma)] - 1/T$ was depicted in Fig. 4. For the given strain rate conditions, $Q_{act}$ can be obtained by differentiating Eqs. (6), as shown in Eqs. (8). From Fig. 4, it can be easily calculated the value of $n_2$ as 5.2392 and $Q_{act}$ as 136.182 J/mol.

$$ln(\dot{\varepsilon}) = n\,ln\left[sinh(\alpha\sigma)\right]+ln(A)-\frac{Q}{RT}\,; \tag{6}$$

$$\frac{\partial\, ln\,\dot{\varepsilon}}{\partial\, ln\left[sinh(\alpha\sigma)\right]} = n\,; \tag{7}$$

$$\frac{\partial\, ln\left[sinh(\alpha\sigma)\right]}{\partial(1/T)} = \frac{Q_{act}}{nR}\,. \tag{8}$$

Step 3: On the basis of the solutions of $Q_{act}$ and $\alpha$, the relationship of $Z$ parameter and flow stress can be obtained in Fig. 5. For the all stress level, stress exponent $n$ and $A$ can be calculated by the slope and intercept of the line, as 5.2212 and $6.1192 \times 10^9$, respectively. Through the above fitting steps, stress exponent $n$ was calculated as 6.694, 5.2392 and 5.2212. It is obvious that $n$ keeps steady in three steps, indicating that successive approximation method is effectively to obtain accurate stress exponent value.

$$ln(Z) = n\,ln\left[sinh(\alpha\sigma)\right]+ln(A)\,. \tag{9}$$

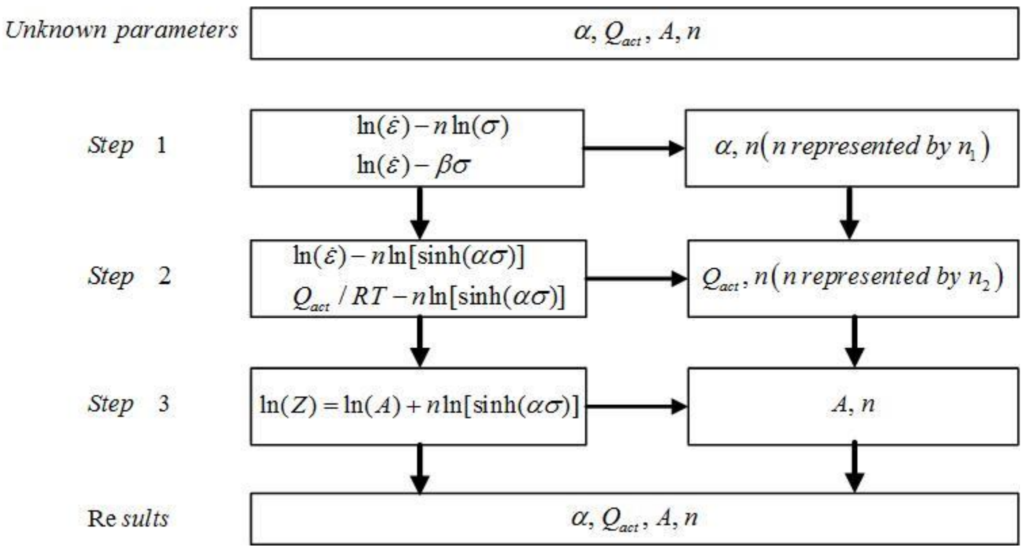


Fig. 2 Steps of successive approximation method for solution of stress exponent $n$

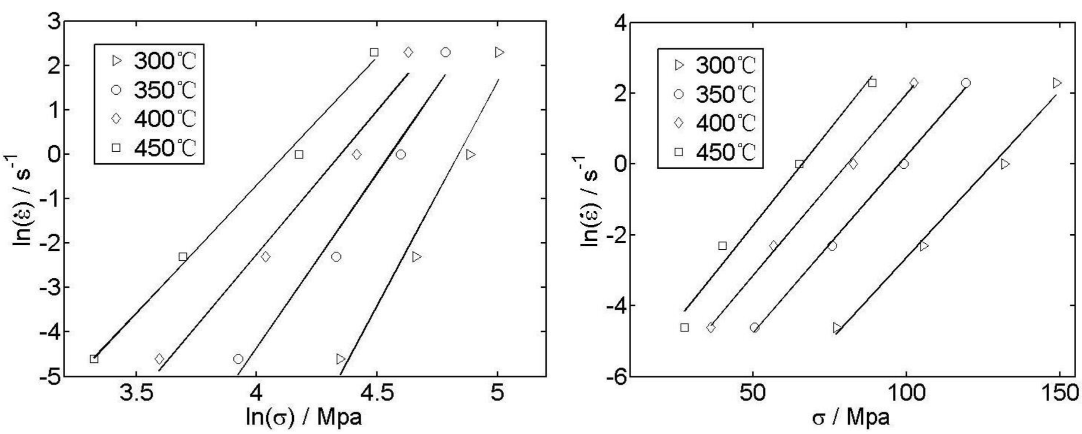


a b

Fig. 3 Relationships between: a - $ln(\dot{\varepsilon})$ and $ln(\sigma)$; b - $ln(\dot{\varepsilon})$ and $\sigma$

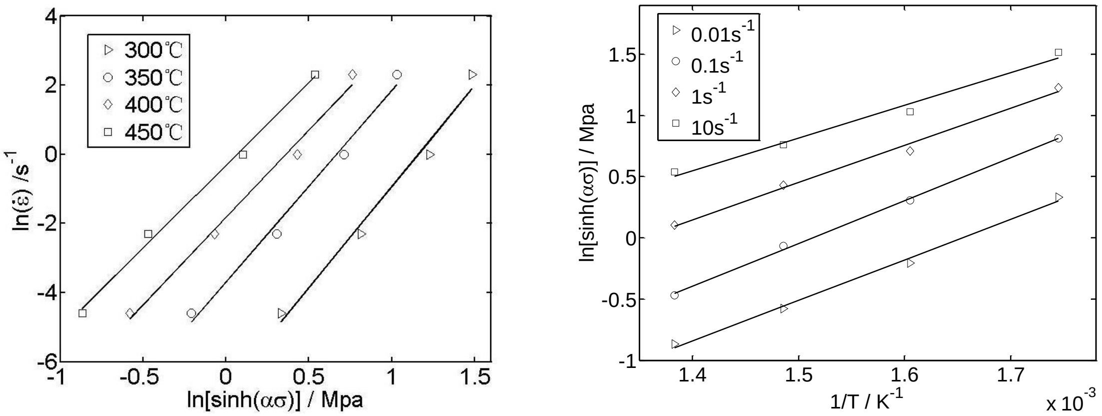


a b

Fig. 4 Relationships between: a - $ln(\dot{\varepsilon})$ and $ln[sinh(\alpha\sigma)]$; b - $ln[sinh(\alpha\sigma)]$ and $1/T$

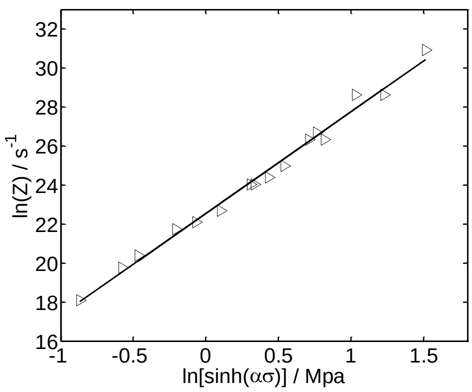


Fig. 5 Relationships between $ln(Z)$ and $ln[sinh(\alpha\sigma)]$

3.2. Constitutive equation considering strain compensation

Normal Arrhenius constitutive equation can only be used to describe the effect of strain rate and temperature on flow stress, especially peak flow stress. However, as can be seen from Fig. 1, the change of strain will cause changes in flow stress, while the relationship between material parameters and strain was not considered in Eq. (10).

$$\sigma = \frac{1}{\alpha} ln\left\{ \left(\frac{Z}{A}\right)^{1/n} + \left[ \left(\frac{Z}{A}\right)^{2/n} + 1 \right]^{1/2} \right\}. \tag{10}$$

In order to obtain a constitutive equation considering strain compensation, the values of material parameters ($ln(A)$, $\alpha$, $\beta$, $n$ and $Q_{act}$) were calculated under different strains(0.05 0.1 0.15 0.2 0.3 0.4 0.5 0.6). The relationship between $ln(A)$, $\alpha$, $\beta$, $n$, $Q_{act}$ and true strain can be polynomial fitted in Fig. 6 and results are given in Eq. (11) and Table 1.

$$\left.\begin{aligned}
ln(A) &= a_0 + a_1\varepsilon + a_2\varepsilon^2 + a_3\varepsilon^3 + a_4\varepsilon^4 + a_5\varepsilon^5;\\
\alpha &= b_0 + b_1\varepsilon + b_2\varepsilon^2 + b_3\varepsilon^3 + b_4\varepsilon^4 + b_5\varepsilon^5;\\
\beta &= c_0 + c_1\varepsilon + c_2\varepsilon^2 + c_3\varepsilon^3 + c_4\varepsilon^4 + c_5\varepsilon^5;\\
n &= d_0 + d_1\varepsilon + d_2\varepsilon^2 + d_3\varepsilon^3 + d_4\varepsilon^4 + d_5\varepsilon^5;\\
Q_{act} &= e_0 + e_1\varepsilon + e_2\varepsilon^2 + e_3\varepsilon^3 + e_4\varepsilon^4 + e_5\varepsilon^5.
\end{aligned}\right\} \tag{11}$$

From Fig. 6, it is obvious that the values of material parameters are sensitive to the variation of true strain. Therefore, the Arrhenius constitutive equation should be modified and the effect of strain on the material parameters should also be taken into consideration. The modified Arrhenius constitutive equations are shown in Eq. (10) and Eqs. (11).

3.3. Error analysis

In order to verify the accuracy of the constitutive equation considering strain compensation, comparisons between calculated flow stress from constitutive equation and experimented results are shown in Fig. 7. In order to quantitatively analyze the accuracy of the fitting, the error $\lambda$ between the calculated stress ($\sigma_c$) by modified Arrhenius constitutive equation and experimented stress ($\sigma_e$) is defined in Eq. (12):

$$\lambda = \frac{|\sigma_c - \sigma_e|}{\sigma_e} \times 100\% . \tag{12}$$

From Fig. 7, it can be easily found that calculated results from the modified Arrhenius constitutive equations agree well with the experimented results and the maximum error is 7.11%, which locates at 300 and 1 $s^{-1}$ when the true strain is 0.05. Therefore, the strain-compensated Arrhenius constitutive equation can be used to predict the flow stress during hot plastic deformation for 7055 aluminum alloy.

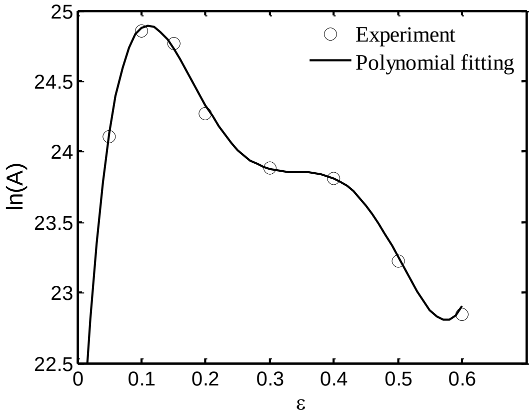


a

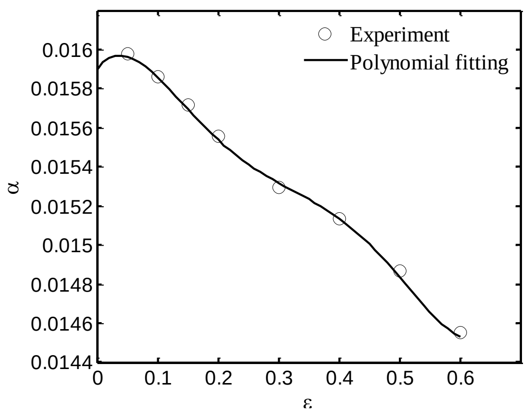


b

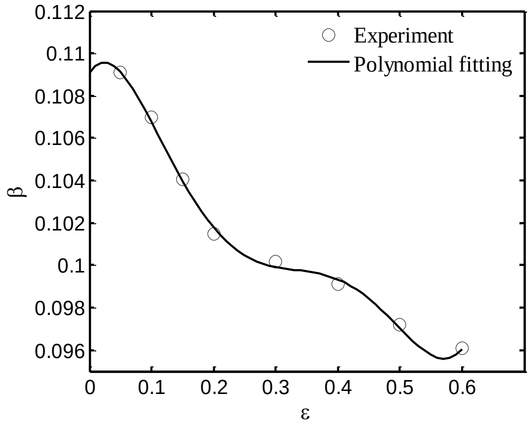


c

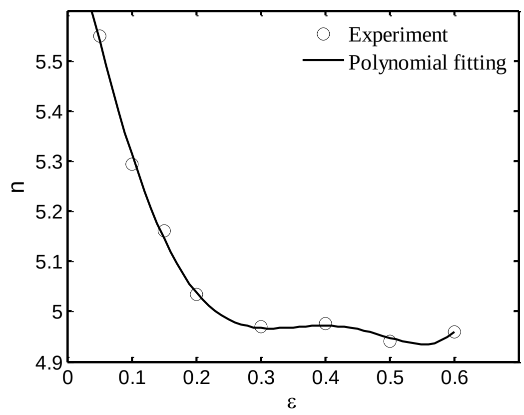


d

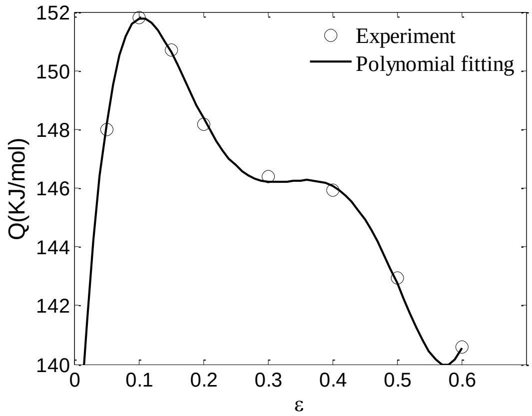


e

Fig. 6 Relationships between: $ln(A)$, $\alpha$, $\beta$, $n$, $Q_{act}$ and strain by polynomial fit

Table 1

Polynomial fit results of material parameters

| ln(*A*) | | $\alpha$ | | $\beta$ | | $n$ | | $Q_{act}$ | |
|---|---|---|---|---|---|---|---|---|---|
| $a_0$ | 21.4 | $b_0$ | 0.0159 | $c_0$ | 0.1091 | $d_0$ | 5.8066 | $e_0$ | 134 |
| $a_1$ | 83.8 | $b_1$ | 0.004 | $c_1$ | 0.0427 | $d_1$ | -5.4663 | $e_1$ | 443 |
| $a_2$ | -697.8 | $b_2$ | -0.0672 | $c_2$ | -1.0683 | $d_2$ | 0.1832 | $e_2$ | -3812 |
| $a_3$ | 2441.7 | $b_3$ | 0.2738 | $c_3$ | 4.9177 | $d_3$ | 68.2738 | $e_3$ | 13652 |
| $a_4$ | -3859.8 | $b_4$ | -0.4731 | $c_4$ | -8.9452 | $d_4$ | -166.0832 | $e_4$ | -21936 |
| $a_5$ | 2253.8 | $b_5$ | 0.2906 | $c_5$ | 5.6967 | $d_5$ | 117.5818 | $e_5$ | 12952 |

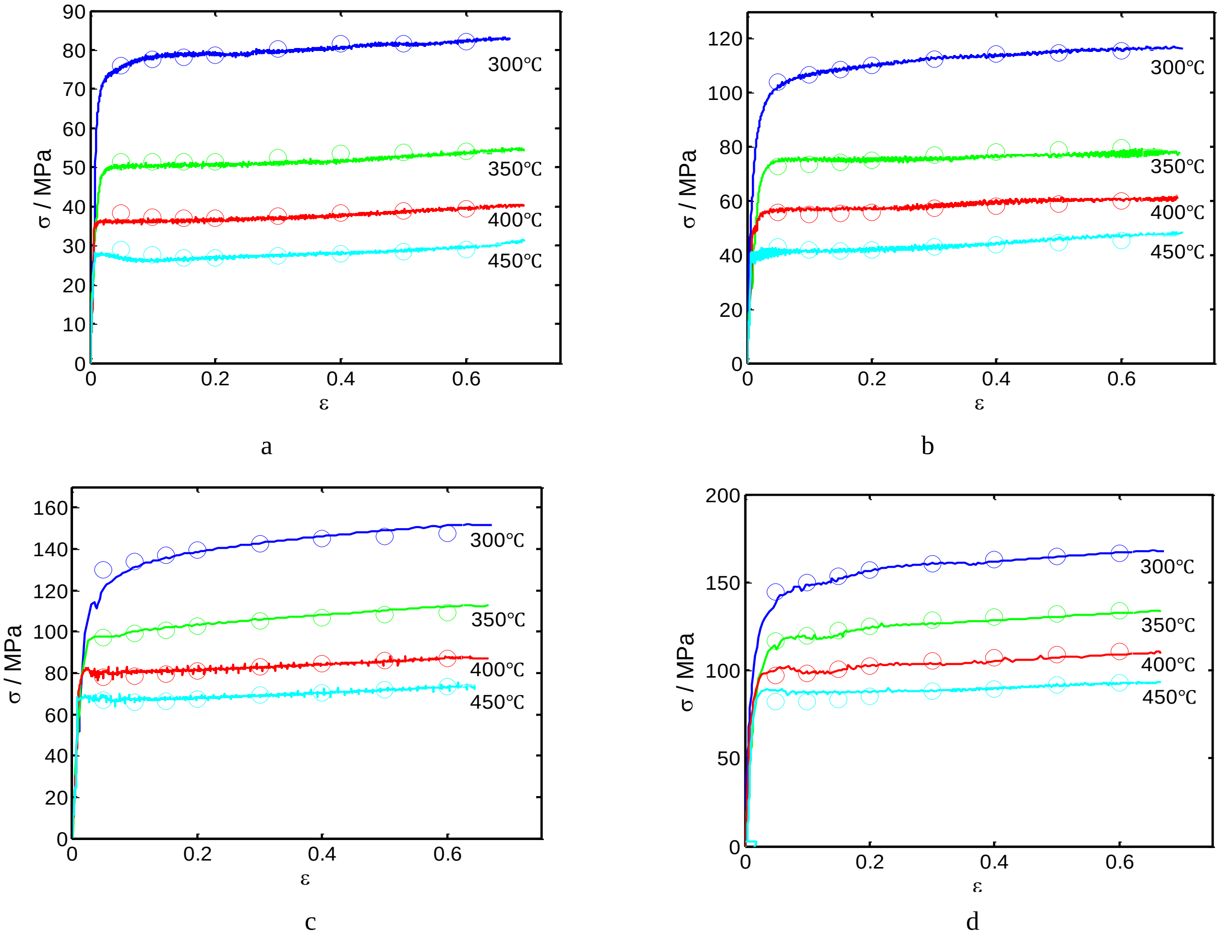


Fig. 7 Comparisons between calculated and experimented flow stress: a - $\dot{\varepsilon}$ = 0.01 $s^{-1}$; b - $\dot{\varepsilon}$ = 0.1 $s^{-1}$; c - $\dot{\varepsilon}$ = 1 $s^{-1}$; c - $\dot{\varepsilon}$ = 10 $s^{-1}$

## 4. Conclusions

1. True stress-strain curves of 7055 aluminum alloy consist of two processes: work hardening and dynamic softening. It is obvious that the peak stress locates at the position of small strain and the flow stress increases with the increase of strain rate and decreases with the increase of temperature.

2. Through the three fitting steps, stress exponent *n* keeps steady, indicating that successive approximation method is effectively to obtain accurate stress exponent value.

3. The Zener-Hollomon parameter only describes the relationship between flow stress and strain rate and temperature, while the change of strain also influences flow stress. The relationship between material parameters in Arrhenius equation and strain was established by polynomial fitting.

4. A modified Arrhenius constitutive equation considering strain compensation was obtained and the validity was examined over all the temperatures and strain rates by the comparison of the experimental results, the maximum error is 7.11%.


## Acknowledgements

This research was funded by National Key Basic Research Development Plan of China (NO.2012CB619505), National Natural Science Foundation of China (No.51405520), the State Key Laboratory of High Performance Complex Manufacturing of China (No.zzyjkt2013-06B) and Key Projects in the National Science & Technology Pillar Program (No.2014BAF12B01).


## References


1. **Kaibyshev, R.; Sakai, T.; Musin, F. et al.** 2001. Superplastic behavior of a 7055 aluminum alloy, Scripta Materialia 45(12): 1373-1380. http://dx.doi:10.1016/S1359-6462(01)01172-1.
2. **Li, Xing-dan** 1994. Development of commercial aircraft aluminum alloy structural materials, Shanghai Nonferrous Metals 15(3): 160-168.
3. **Lin, Y.C.; Chen, X.M.** 2011. A critical review of experimental results and constitutive descriptions for metals and alloys in hot working, Materials & Design 32(4): 1733-1759. http://dx.doi:10.1016/j.matdes.2010.11.048.
4. **Liang, R.; Khan, A.S.** 1999. A critical review of experimental results and constitutive models for BCC and FCC metals over a wide range of strain rates and temperatures, International Journal of Plasticity 15(9): 963-980. http://dx.doi:10.1016/j.matdes.2010.11.048.
5. **Chen, K.; Liu, H.; Zhang, Z. et al.** 2003. The improvement of constituent dissolution and mechanical properties of 7055 aluminum alloy by stepped heat treatments, Journal of Materials Processing Technology 142(1): 190-196.

http://dx.doi:10.1016/S0924-0136(03)00597-1.
6. **Mondal, C.; Mukhopadhyay, A.K.; Raghu, T. et al.** 2007. Tensile properties of peak aged 7055 aluminum alloy extrusions, Materials Science and Engineering: A 454: 673-678.
http://dx.doi:10.1016/j.msea.2006.10.138.
7. **Yan, L.; Jian, S.; Li, Z. et al.** 2013. Effect of deformation temperature on microstructure and mechanical properties of 7055 aluminum alloy after heat treatment, Transactions of Nonferrous Metals Society of China 23(3): 625-630.
http://dx.doi:10.1016/S1003-6326(13)62508-X.
8. **Dixit, M.; Mishra, R.S.; Sankaran, K.K.** 2008. Structure–property correlations in Al 7050 and Al 7055 high-strength aluminum alloys, Materials Science and Engineering: A 478(1): 163-172.
http://dx.doi:10.1016/j.msea.2007.05.116.
9. **Chen, J.; Zhen, L.; Yang, S. et al.** 2009. Investigation of precipitation behavior and related hardening in AA 7055 aluminum alloy, Materials Science and Engineering: A 500(1): 34-42.
http://dx.doi:10.1016/j.msea.2008.09.065.
10. **Lin, Y.C.; Chen, M.S.; Zhong, J.** 2008. Constitutive modeling for elevated temperature flow behavior of 42CrMo steel, Computational Materials Science 42(3): 470-477.
http://dx.doi:10.1016/j.commatsci.2007.08.011.
11. **Lin, Y.C.; Chen, M.S.; Zhong, J.** 2009. Modeling of flow stress of 42CrMo steel under hot compression, Materials Science and Engineering: A 499(1): 88-92.
http://dx.doi:10.1016/j.msea.2007.11.119.
12. **Zhang, H.; Lin, G.Y.; Peng, D.S. et al.** 2004. Dynamic and static softening behaviors of aluminum alloys during multistage hot deformation, Journal of Materials Processing Technology 148: 245-249.
http://dx.doi:10.1016/j.jmatprotec.2003.12.020.
13. **Yan, L.; Shen, J.; Li, Z. et al.** 2010. Modeling for flow stress and processing map of 7055 aluminum alloy based on artificial neural networks, The Chinese Journal of Nonferrous Metals 20(7): 1296-1301.
14. **Quan, G.; Yu, C.; Liu, Y. et al.** 2014. A comparative study on improved arrhenius-type and artificial neural network models to predict high-temperature flow behaviors in 20MnNiMo alloy, The Scientific World Journal 2014(2014).
http://dx.doi.org/10.1155/2014/108492.
15. **Zhang, C.; Li, X.; Li, D. et al.** 2012. Modelization and comparison of Norton-Hoff and Arrhenius constitutive laws to predict hot tensile behavior of Ti–6Al–4V alloy, Transactions of Nonferrous Metals Society of China 22: s457-s464.
http://dx. doi:10.1016/S1003-6326(12)61746-4.
16. **Li, J.; Li, F.; Cai, J. et al.** 2010. Flow behavior modeling of the 7050 aluminum alloy at elevated temperatures considering the compensation of strain, Materials & Design 42: 369-377.
http://dx.doi:10.1016/S1003-6326(12)61746-4.
17. **Chen, S.; Chen, K.; Le, J.I.A. et al.** 2013. Effect of hot deformation conditions on grain structure and properties of 7085 aluminum alloy, Transactions of Nonferrous Metals Society of China 23(2): 329-334.
http://dx.doi.org/10.1016/S1003-6326(13)62465-6.

Zhang Tao, Wu Yun-xin, Gong Hai, Shi Wen-ze,
Jiang Fang-min

FLOW STRESS BEHAVIOR AND CONSTITUTIVE MODEL OF 7055 ALUMINUM ALLOY DURING HOT PLASTIC DEFORMATION

S u m m a r y

In order to acquire flow characteristics in hot plastic deformation and establish the optimum hot formation processing parameters for 7055 aluminum alloy, the hot compressive flow stress behavior was studied at the temperatures from 300 to 450 and strain rates from 0.01 to 10 $s^{-1}$ on Gleeble-3180 thermo-simulation machine. The stress exponent and activation energy were acquired with successive approximation method by regression analysis. The relationship between material parameters in Arrhenius equation and strain was established by polynomial fitting and a modified Arrhenius constitutive equation considering strain compensation was established. The results show that 7055 aluminum alloy is positive strain rate sensitive material and the flow stress increases with the increase of strain rate and decreases with the increase of temperature. The experimental results agree with the predictive values according to the modified Arrhenius constitutive equation and the maximum error is 7.11%.

**Key words:** 7055 aluminum alloy; hot plastic deformation; successive approximation method; flow stress; modified Arrhenius constitutive equation.

Received September 09, 2015
Accepted September 28, 2016